Bistability in a Driven-Dissipative Superfluid

Ralf Labouvie,[1,2] Bodhaditya Santra,[1] Simon Heun,[1] and Herwig Ott[1]
[1]Department of Physics and Research Center OPTIMAS, Technische Universität Kaiserslautern, 67663 Kaiserslautern, Germany
[2]Graduate School Materials Science in Mainz, Staudinger Weg 9, 55128 Mainz, Germany
(Received 17 July 2015; published 10 June 2016)

We experimentally study a driven-dissipative Josephson junction array, realized with a weakly interacting Bose-Einstein condensate residing in a one-dimensional optical lattice. Engineered losses on one site act as a local dissipative process, while tunneling from the neighboring sites constitutes the driving force. We characterize the emerging steady states of this atomtronic device. With increasing dissipation strength γ the system crosses from a superfluid state, characterized by a coherent Josephson current into the lossy site, to a resistive state, characterized by an incoherent hopping transport. For intermediate values of γ, the system exhibits bistability, where a superfluid and an incoherent branch coexist. We also study the relaxation dynamics towards the steady state, where we find a critical slowing down, indicating the presence of a nonequilibrium phase transition.

DOI: 10.1103/PhysRevLett.116.235302

Nonequilibrium steady states (NESS) constitute fixed points of the phase space dynamics of classical and quantum systems [1–3]. They emerge under the presence of a driving force and lie at the heart of transport phenomena such as heat conduction [4–6] or current flow [7–9]. They also naturally appear in open quantum systems [10,11] and are connected to the study of nonequilibrium thermodynamics and nonequilibrium quantum phase transitions [12]. It has been pointed out that engineering open quantum systems can induce a phase space dynamics that drives the quantum system in a pure state by solely dissipative means [13–16]. Controlling and understanding the nonequilibrium steady states of an open many-body quantum system therefore offers new routes for quantum state engineering and out-of-equilibrium quantum dynamics.

In general, the dynamics of an open quantum system is characterized by the competition between the intrinsic unitary dynamics, governed by the Hamilton operator H, and the coupling to the environment, which induces nonunitary time evolution and quantum jumps. These are described by the Lindblad operators $(\hat{R}_i, \hat{R}_i^\dagger)$, which act on the system with rate γ_i, where we use the standard textbook definition [10]. The time evolution of the density matrix ρ in Markov approximation is then described by a master equation in Lindblad form [17],

$$\dot{\rho} = \mathcal{L}(\rho) = -\frac{i}{\hbar}[H,\rho] + \sum_i \frac{\gamma_i}{2}(2\hat{R}_i\rho\hat{R}_i^\dagger - \hat{R}_i^\dagger\hat{R}_i\rho - \rho\hat{R}_i^\dagger\hat{R}_i). \quad (1)$$

NESS are defined by the condition $\mathcal{L}(\rho_{\mathrm{NESS}}) = 0$. The steady state can be a mixed state or a pure state, i.e., $\rho_{\mathrm{NESS}} = |\Psi_{\mathrm{NESS}}\rangle\langle\Psi_{\mathrm{NESS}}|$. When the jump operators do not affect a pure state, such that $\hat{R}_i|\Psi_{\mathrm{NESS}}\rangle = 0$, the state $|\Psi_{\mathrm{NESS}}\rangle$ is called a dark state. Steady states have the peculiar property that they can be attractor states of the phase space dynamics. This is especially interesting for dark states, because it allows for the dissipative creation of a pure quantum state, which is decoupled from the dissipation. The same mechanism also stabilizes the system, as the dissipation always drives it back into the dark state. Engineered dissipation is therefore a way to create robust quantum states.

Here, we investigate the steady states of a driven-dissipative Josephson junction array realized with a Bose-Einstein condensate (BEC) in a one-dimensional optical lattice [18]. The dissipation is implemented as a local particle loss in one site, and the drive is provided by tunneling of atoms from the adjacent sites (Fig. 1).

The experiment is realized with a weakly interacting BEC of 45×10^3 ^{87}Rb atoms in a one-dimensional periodic potential with high occupancy per site [19]. Each site contains a small condensate ($N_0 \approx 700$ atoms in the center of the trap) and all of them are connected via the tunneling

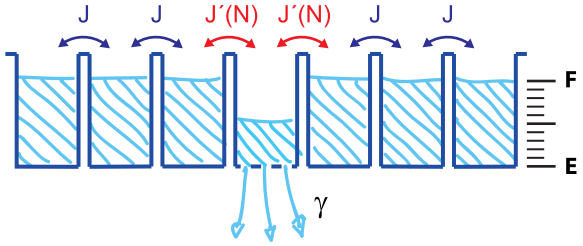

FIG. 1. Schematics of the experiment. One site of an array of superfluids is subject to an incoherent local loss process with rate γ. The coherent tunneling coupling between the reservoir sites is given by J. The coupling to the lossy site is given by $J'(N)$ and depends on the filling level (see text).

coupling J, which is controlled by the height of the optical lattice. Employing a scanning electron microscopy technique [22], we introduce a well-defined local particle loss as a dissipative process in a single site of the system. To set the dissipation strength γ, we adjust the effective intensity of the electron beam [19]. The corresponding jump operator is then given by the bosonic annihilation operator $\hat{a}_m$ (the index m denotes the affected site), acting on all spatial modes of the lossy site with the same dissipation rate γ. A fraction of the lost atoms is ionized by the electron beam and serves as a continuous probe of the occupation of the lossy site. The drive is provided by the large number of full sites left and right. The overall atom loss during a measurement is about 10%, such that we can consider these sites as a superfluid reservoir. Figure 1 shows a sketch of the experimental scenario. Related systems based on dissipative Bose-Hubbard models have been studied theoretically in Refs. [23–26].

At the beginning of each experimental sequence, we initialize different starting conditions by optionally emptying the lossy site. Upon continuous dissipation, a steady state is established on a time scale of several tens of milliseconds and the losses are balanced by the refilling dynamics. At the end of the experimental sequence we freeze out and probe the final density distribution in a deep lattice. Figure 2(a) shows the resulting filling level of the lossy site in the steady state in dependence of the dissipation rate γ. The two data sets correspond to an initially full site (blue points) and empty site (red points). For small values of γ, both initial conditions lead to a completely full site in the steady state. For large dissipation, the lossy site is almost empty in both cases. The most prominent feature appears in between: the appearance of bistability. Starting from an empty site leads to a different filling level in the steady state compared to starting from a full site. The inset in Fig. 2(a) shows the two different trajectories, clearly displaying the two coexisting steady states. As will be explained in detail below, we refer to the steady states with unity filling as the superfluid branch (SF) and with finite population difference as the lower branch (LB).

To analyze the properties of the steady states we evaluate the current of atoms into the lossy site. The temporal evolution of the atom number in that site is given by

$$\dot{N}(t) = -\gamma N(t) + I(t), \tag{2}$$

where $N(t)$ is the number of atoms in the lossy site and $I(t)$ is the current from the reservoir sites. The steady state has to fulfil $\dot{N} = 0$, such that the steady-state current is given by $I_S = \gamma N_S$, where the subscript denotes the steady-state value. This allows us to convert the filling level shown in Fig. 2(a) into the current plot shown in Fig. 2(b). Converting the atom number difference in chemical potential difference [27], we can also extract the current-voltage characteristics for the steady states [Fig. 2(c)].

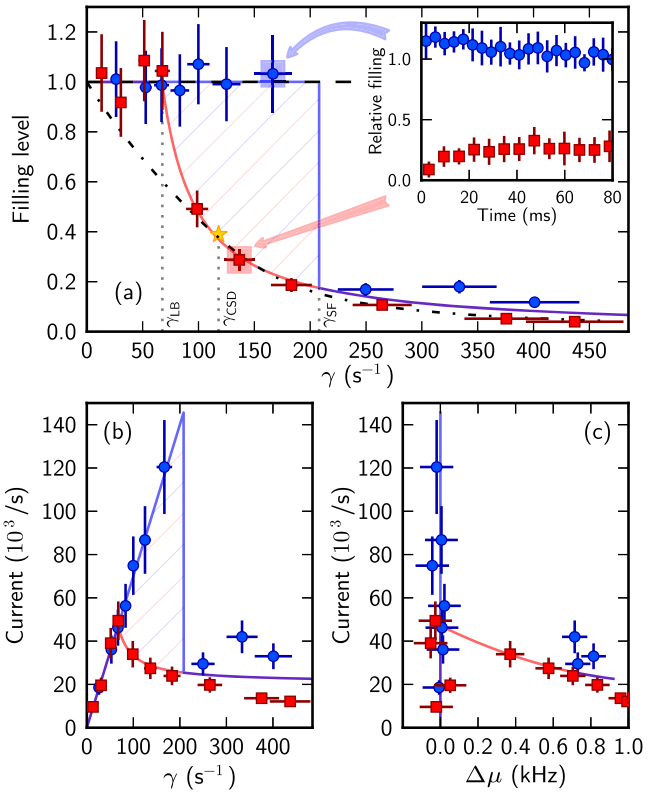

FIG. 2. (a) Steady-state filling level of the lossy site in dependence of the dissipation strength γ for an initially full (blue circles) and empty (red squares) site. The tunneling coupling between the sites is $J/\hbar = 230$ s^{-1}. The hatched area indicates the region of bistability (the transparent, solid lines are a guide to the eye). The dashed and dash-dotted black lines are results of theoretical models as discussed in the main text. γ_{LB}, γ_{CSD}, and γ_{SF} denote critical values of the dissipation, obtained from the data, and are also explained in the main text. Inset: dynamical evolution of the system into the steady state within the bistable region for both initial conditions. (b) Steady-state current into the lossy site in dependence of γ. (c) For small values of $\Delta\mu$, the current-voltage characteristics display the typical behavior of a superconductor.

We now discuss the nature of the different steady states that we observe. For small dissipation, when the filling is always equal to 1, the current into the lossy site is exactly linear to the applied dissipation [Fig. 2(b)]. This is remarkable, as the dissipation is externally applied and it is not *a priori* obvious that the current response induced by the dissipation exactly balances the losses. Because there is no difference in atom number between the sites in this regime, the current cannot be driven by a difference in chemical potential. Instead, it can only be driven by a phase gradient between the sites, thus constituting a supercurrent. This is also visible in the current-voltage characteristics for the steady states [Fig. 2(c)], which show the characteristic behavior

of a superconductor: a finite current in the absence of an applied voltage.

The appearance of a supercurrent can be directly understood from an effective Josephson model

$$i\hbar\frac{\partial\psi_n}{\partial t} = -J(\psi_{n-1}+\psi_{n+1}) + U|\psi_n|^2\psi_n + i\frac{\gamma}{2}\psi_n\delta_{nm}, \quad (3)$$

where J is the tunneling coupling, U is the on-site interaction, and m denotes the lossy site. In this mean-field version of the problem, the losses are implemented as an imaginary potential [28]. This model indeed supports a steady-state solution with unity filling at each site and a phase difference of $\sin(\Delta\Phi) = \hbar\gamma/(4J)$ between all adjacent sites [shown as the dashed black line in Fig. 2(a)]. The observed supercurrent is therefore a steady state under the combined action of the unitary dynamics and external dissipation. The theoretical model predicts that the steady state is a pure state, corresponding to a Bloch state with finite quasimomentum q. For small values of γ, the system reaches a superfluid steady state irrespective of the initial condition. These steady states are therefore attractor states of the phase space dynamics and their generation is an example for dissipative quantum state engineering. A related situation has been theoretically studied for a three well system in Ref. [29]. There it was found that the interplay between dissipation and interaction leads to a well-defined relative phase between the three wells.

The Josephson model predicts a maximum possible supercurrent of $I_{\mathrm{crit}} = 4NJ/\hbar$. In our experiment, we only reach about 25% of this value. This indicates that the validity of the Josephson model breaks down above a critical dissipation strength [denoted by γ_{SF} in Fig. 2(a)]. Indeed, this does not come as a surprise, as the full microscopic model of our experiment goes beyond the validity of Eq. (3). During the dynamics, each site can support transverse excitations and phase fluctuations, thus rendering the supercurrent unstable. For a dissipation strength below the critical value γ_{SF}, however, a clear supercurrent can be observed, in analogy to an electric supercurrent in a voltage biased Josephson junction [30]. We therefore refer to this class of steady states as the superfluid branch.

For a dissipation strength exceeding γ_{SF}, all steady states are characterized by a strongly reduced population in the lossy site, corresponding to a finite voltage drop. The coherence to the neighboring site is destroyed and the transport of particles is realized by incoherent hopping processes. As the tunneling coupling reduces with increasing population imbalance (see below), this regime exhibits negative differential conductivity, as observed previously [27]. Because of the absence of superfluidity, this regime can be modeled with an effective single particle model, including local phase noise due to collisions, losses, and a filling dependent effective tunneling coupling [19]. The result is shown in Fig. 2(a) as dash-dotted black line. For better comparison with the experiment, we plot the solution of the model for the whole range of γ. Note that this model does not include the interaction between the atoms and therefore does not support superfluid transport. For $\gamma > \gamma_{\mathrm{SF}}$, the phase noise and the dissipation rates completely dominate the dynamics and we refer to this class of steady states as normal.

The bistable region ($\gamma_{\mathrm{LB}} < \gamma < \gamma_{\mathrm{SF}}$) supports superfluid steady states and steady states with finite population difference. Bistability occurs in various physical systems, e.g., optics [31] and electronic tunneling devices [32], and requires an intrinsic nonlinearity in the system. In our experiment, the nonlinearity has its origin in the interaction energy between the atoms, which leads to a filling dependent on-site energy. Different filling therefore corresponds to a difference in chemical potential. Atoms tunneling into the lossy site are therefore either off-resonantly coupled to a condensate with reduced atom number (provided a condensate fraction exists at all) or can tunnel resonantly into radially excited states. In this case, however, an additional Franck-Condon factor comes into play that leads to a reduced tunneling coupling $J'(N) < J$. The availability of these single particle states in the central sites prevents the system from self-trapping [27]. Both effects suppress the transport of particles in the central site, thus giving rise to bistability.

The precise microscopic modeling of the bistability region is challenging. We first note that the scaling of γ_{LB} with J follows a power law with an exponent of 1.7(2) [Fig. 3(a)]. This quadratic dependence suggests that the steady states in the LB have an incoherent component and the transport can no longer be provided by a supercurrent alone. Moreover, the LB connects to the normal regime, where the transport is completely incoherent. Therefore, a

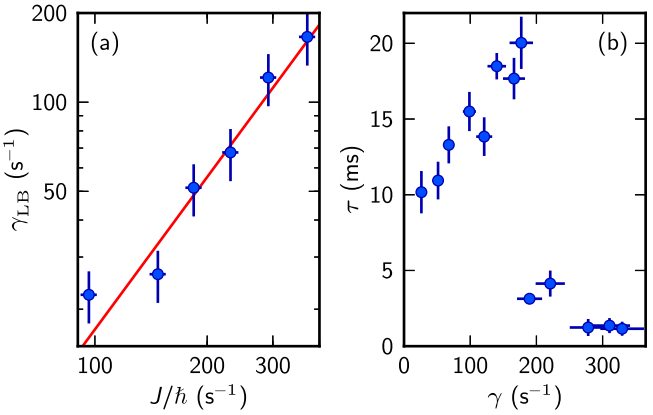

FIG. 3. (a) Critical dissipation rate γ_{LB} in dependence of the tunneling rate. We find a power law dependence with an exponent 1.7(2). This corresponds to a transition from a coherent to an incoherent process at which the internal rates become proportional to J^2. (b) Time τ in which the steady state is reached for different dissipation rates at $J/\hbar = 290\ \mathrm{s}^{-1}$. Within the bistable region τ is increasing, which is known as critical slowing down.

realistic model has to merge the ingredients of both models introduced above: (i) superfluid transport, (ii) nonlinear tunneling coupling, (iii) phase noise, and (iv) dissipation. In addition, (v) it has to exclude self-trapping in order to correctly account for the multimode level structure in each well. Such a model is practically not feasible due to the many spatial modes and high atom number. From a qualitative point of view, the appearance of bistability can be explained on a mean-field level using an effective single site Hamiltonian with pumping term [26,31]. However, we could not find quantitative agreement within the parameter range. The qualitative understanding of the appearance of bistability is clear: for a given dissipation strength, the superfluid response is strong enough to preserve unit filling, while the reduced tunneling current for lower filling cannot compete with the losses. This is also visible in Fig. 2(a), where the two simplified models provide the correct boundaries for the steady states.

We close the discussion by analyzing the dynamics towards the steady state and studying the nature of the transition from normal to superfluid transport. Starting from an initially empty site [red points in Fig. 2(a)] we measure the time scale τ in which the steady state is established. In Fig. 3(b), we show τ in dependence of the dissipation rate. Increasing the dissipation rate, τ increases accordingly, reaching a maximum value and drastically dropping at a critical dissipation strength γ_{CSD}. Note that Fig. 3(b) is measured for a different value of J. This is reminiscent of a critical slowing down [33] and appears well within the bistable region [indicated with a star in Fig. 2(a)]. We assume that this critical slowing down originates form the phase transition from a normal gas to an out-of-equilibrium condensate in the lossy site. Without dissipation, the conditions for Bose-Einstein condensation are already reached for a filling level of 10% and one would expect the appearance of a condensate throughout the LB. In the presence of dissipation, however, the formation of a condensate competes with the losses, thus modifying or even inhibiting a phase transition. Three observations support the presence of a phase transition. (i) The current in the LB for $\gamma < \gamma_{\mathrm{CSD}}$ is higher than any current we observe for the bare refilling dynamics without dissipation. This suggests a partially superfluid transport. (ii) This is in accordance with the effective single particle model [dash-dotted line in Fig. 2(a)], which starts to deviate from the experimental data around γ_{CSD}, thus indicating the onset of superfluid transport. (iii) The width of the radial density distribution in the lossy site is slightly reduced for $\gamma < \gamma_{\mathrm{CSD}}$ despite the higher atom number. This suggests a condensation process in the lossy site.

Because all involved time scales, such as the dissipation rate γ, the effective tunneling coupling $J'(N)$, and the collision rate [27] are of similar magnitude, such a condensation process is likely to be a nonequilibrium process, as observed, e.g., in exciton-polariton condensates [34]. In the future, a detailed study of the atom number fluctuations and the scaling laws around γ_{CSD} will offer new ways to characterize and classify such nonequilibrium phase transitions with a high level of control.

All previously obtained results can be summarized in a phase diagram (Fig. 4), where the steady states are classified in three regimes. For small dissipation rates and high tunneling couplings the system ends up in a superfluid state (blue shaded area) independent from the starting condition. Adjacent is the bistable region (hatched area) in which the system stays superfluid starting from a full site but ends up in a steady state with finite atom number difference when starting from an empty site. Further increasing the dissipation rate connects the bistable region to the normal region (red shaded area) characterized by low filling and incoherent hopping transport. The data points are the corresponding boundaries for γ_{LB}, γ_{CSD}, and γ_{SF} obtained from the analysis of Figs. 2(a) and 3(b) for different tunneling couplings, respectively. Within the bistable region, we find a critical slowing down (indicated by the yellow line), which we interpret as an out-of-equilibrium condensation process in the LB. In Ref. [12], it has been studied how nonequilibrium noise affects the normal to superconductor phase transition in a single Josephson junction, which is described by a simple phase boundary. In the present work, the nonlinear tunneling coupling prevents the existence of a simple phase boundary, but introduces a region of bistability between the superfluid and normal steady states. The rich phase

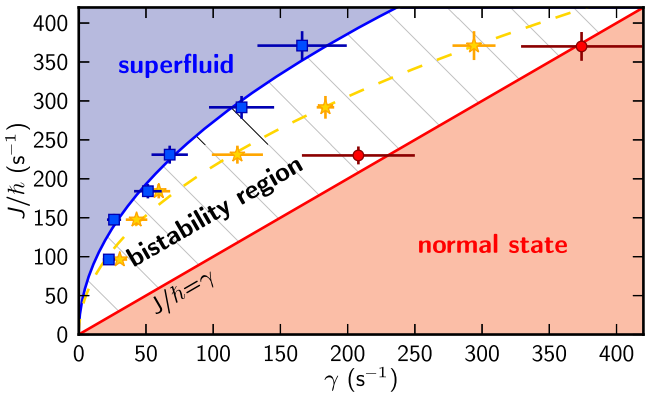

FIG. 4. Phase diagram of the steady states. The blue shaded area marks the region where the lossy site is always filled independent from the initial condition and a supercurrent is induced. The red shaded area denotes the region of normal steady states, where the system ends up in an almost empty site with an incoherent hopping transport, driven by the difference in chemical potential. In between (hatched area) the system is bistable, resulting in different steady states depending on the initial conditions. The blue squares (red dots, yellow stars) denote γ_{LB} (γ_{SF}, γ_{CSD}). The blue line is the fit from Fig. 3(a), the yellow line is a guide to the eye, and the red line marks the boundary, where the dissipation strength γ equals the coherent coupling $J/\hbar$.

diagram promotes the dissipative Josephson junction as a versatile tool for atomtronics applications. The transport properties can be switched between different regimes and tuned over a large parameter range. They can even be varied dynamically, thus taking advantage of the intrinsic hysteresis in the system.

Engineering a local loss process in an ultracold quantum gas, we have achieved a high level of control over an open many-body quantum system. This has allowed us to study and characterize the steady-state phase diagram of a driven-dissipative superfluid and to observe bistability. Our results manifest the high potential of open system control in ultracold quantum gases. Closely related to our experiment is the appearance of a superfluid branch and a dissipative branch in biased Josephson junctions [35]. In the future, studying the fluctuations around the steady states will be a tool to look at generalized dissipation fluctuation theorems for nonequilibrium systems [36]. The exploration of quantum phases with the help of competing dissipation mechanisms [37], the quest for complex many-body dark states [13,14,38–40], and the investigation of nonequilibrium phase transitions [41] make open system control a paradigm for future quantum research.

We thank Michael Fleischhauer, Matthias Moos, Eugene Demler, Axel Pelster, Sandro Wimberger, and Jacob Sherson for fruitful discussions. This work was supported by the Deutsche Forschungsgemeinschaft within the Graduate School of Excellence MAINZ.

[1] S. Strogatz, *Nonlinear Dynamics and Chaos* (Westview Press, Boulder, 2014).
[2] H. Spohn and J. L. Lebowitz, Commun. Math. Phys. **54**, 97 (1977).
[3] G. Gallavotti and E. G. D. Cohen, Phys. Rev. Lett. **74**, 2694 (1995).
[4] K. Schwab, E. A. Henriksen, J. M. Worlock1, and M. L. Roukes, Nature (London) **404**, 974 (2000).
[5] D. Segal, A. Nitzan, and P. Hänggi, J. Chem. Phys. **119**, 6840 (2003).
[6] T. S. Komatsu, N. Nakagawa, S.-i. Sasa, and H. Tasaki, Phys. Rev. Lett. **100**, 230602 (2008).
[7] W. Kohn and J. M. Luttinger, Phys. Rev. **108**, 590 (1957).
[8] A. Pecchia and A. Di Carlo, Rep. Prog. Phys. **67**, 1497 (2004).
[9] K. S. Novoselov, A. K. Geim, S. V. Morozov, D. Jiang, M. I. Katsnelson, I. V. Grigorieva, S. V. Dubonos, and A. A. Firsov, Nature (London) **438**, 197 (2005).
[10] H.-P. Breuer and F. Petruccione, *The Theory of Open Quantum Systems* (Oxford University Press, Oxford, 2002).
[11] A. J. Daley, Adv. Phys. **63**, 77 (2014).
[12] E. G. D. Torre, E. Demler, T. Giamarchi, and E. Altman, Nat. Phys. **6**, 806 (2010).
[13] S. Diehl, A. Micheli, A. Kantian, B. Kraus, H. P. Büchler, and P. Zoller, Nat. Phys. **4**, 878 (2008).
[14] F. Verstraete, M. M. Wolf, and J. I. Cirac, Nat. Phys. **5**, 633 (2009).
[15] J. T. Barreiro, M. Müller, P. Schindler, D. Nigg, T. Monz, M. Chwalla, M. Hennrich, C. F. Roos, P. Zoller, and R. Blatt, Nature (London) **470**, 486 (2011).
[16] M. K. Pedersen, J. J. W. H. Sørensen, M. C. Tichy, and J. F. Sherson, New J. Phys. **16**, 113038 (2014).
[17] G. Lindblad, Commun. Math. Phys. **48**, 119 (1976).
[18] F. S. Cataliotti, S. Burger, C. Fort, P. Maddaloni, F. Minardi, A. Trombettoni, A. Smerzi, and M. Inguscio, Science **293**, 843 (2001).
[19] See Supplemental Material http://link.aps.org/supplemental/10.1103/PhysRevLett.116.235302, which includes Refs. [20–21], for details on the experimental setup, the calibration of the dissipation rate, and a brief description of the single particle model.
[20] T. Gericke, P. Würtz, D. Reitz, C. Utfeld, and H. Ott, Appl. Phys. B **89**, 447 (2007).
[21] P. Würtz, T. Gericke, A. Vogler, and H. Ott, New J. Phys. **12**, 065033 (2010).
[22] B. Santra and H. Ott, J. Phys. B **48**, 122001 (2015).
[23] P. Barmettler and C. Kollath, Phys. Rev. A **84**, 041606(R) (2011).
[24] D. Witthaut, F. Trimborn, H. Hennig, G. Kordas, T. Geisel, and S. Wimberger, Phys. Rev. A **83**, 063608 (2011).
[25] A. LeBoité, G. Orso, and C. Ciuti, Phys. Rev. Lett. **110**, 233601 (2013).
[26] I. Vidanović, D. Cocks, and W. Hofstetter, Phys. Rev. A **89**, 053614 (2014).
[27] R. Labouvie, B. Santra, S. Heun, S. Wimberger, and H. Ott, Phys. Rev. Lett. **115**, 050601 (2015).
[28] G. Barontini, R. Labouvie, F. Stubenrauch, A. Vogler, V. Guarrera, and H. Ott, Phys. Rev. Lett. **110**, 035302 (2013).
[29] J. A. Dunningham and K. Burnett, J. Phys. B **33**, 3807 (2000).
[30] A. Steinbach, P. Joyez, A. Cottet, D. Esteve, M. H. Devoret, M. E. Huber, and J. M. Martinis, Phys. Rev. Lett. **87**, 137003 (2001).
[31] P. D. Drummond and D. F. Walls, J. Phys. A **13**, 725 (1980).
[32] V. J. Goldman, D. C. Tsui, and J. E. Cunningham, Phys. Rev. Lett. **58**, 1256 (1987).
[33] R. Bonifacio and P. Meystre, Opt. Commun. **29**, 131 (1979).
[34] M. Richard, J. Kasprzak, R. André, R. Romestain, L. S. Dang, G. Malpuech, and A. Kavokin, Phys. Rev. B **72**, 201301 (2005).
[35] G. Schön and A. D. Zaikin, Phys. Rep. **198**, 237 (1990).
[36] J. Prost, J.-F. Joanny, and J. M. R. Parrondo, Phys. Rev. Lett. **103**, 090601 (2009).
[37] N. Lang and H. P. Büchler, Phys. Rev. A **92**, 012128 (2015).
[38] B. Kraus, H. P. Büchler, S. Diehl, A. Kantian, A. Micheli, and P. Zoller, Phys. Rev. A **78**, 042307 (2008).
[39] S. Diehl, E. Rico, M. A. Baranov, and P. Zoller, Nat. Phys. **7**, 971 (2011).
[40] G. Kordas, S. Wimberger, and D. Witthaut, Europhys. Lett. **100**, 30007 (2012).
[41] F. Brennecke, R. Mottl, K. Baumann, R. Landig, T. Donner, and T. Esslinger, Proc. Natl. Acad. Sci. U.S.A. **110**, 11763 (2013).